The Representation of Snow in Land Surface Schemes: Results from PILPS 2(d)

A. G. SLATER,[a,c] C. A. SCHLOSSER,[b] C. E. DESBOROUGH,[c] A. J. PITMAN,[c] A. HENDERSON-SELLERS,[d] A. ROBOCK,[e] K. YA. VINNIKOV,[f] K. MITCHELL,[g] A. BOONE,[h] H. BRADEN,[i] F. CHEN,[g] P. M. COX,[j] P. DE ROSNAY,[k] R. E. DICKINSON,[l] Y.-J. DAI,[m] Q. DUAN,[n] J. ENTIN,[j] P. ETCHEVERS,[h] N. GEDNEY,[o] YE. M. GUSEV,[p] F. HABETS,[h] J. KIM,[q] V. KOREN,[n] E. A. KOWALCZYK,[r] O. N. NASONOVA,[p] J. NOILHAN,[h] S. SCHAAKE,[n] A. B. SHMAKIN,[s] T. G. SMIRNOVA,[a] D. VERSEGHY,[t] P. WETZEL,[u] Y. XUE,[v] Z.-L. YANG,[l] AND Q. ZENG[m]

[a] *CIRES, University of Colorado, Boulder, Colorado*
[b] *Center for Ocean–Land–Atmosphere Studies, Calverton, Maryland*
[c] *Department of Physical Geography, Macquarie University, Sydney, Australia*
[d] *Australian Nuclear Science and Technology Organisation, Sydney, Australia*
[e] *Department of Environmental Sciences, Rutgers University, New Brunswick, New Jersey*
[f] *Department of Meteorology, University of Maryland, College Park, College Park, Maryland*
[g] *Environmental Modeling Center, NOAA/NCEP, Camp Springs, Maryland*
[h] *Météo-France/CNRM, Toulouse, France*
[i] *German Meteorological Service, Braunschweig, Germany*
[j] *Hadley Centre for Climate Prediction and Research, Bracknell, Berkshire, United Kingdom*
[k] *Laboratoire de Meteorologie Dynamique du CNRS, Paris, France*
[l] *Institute of Atmospheric Physics, The University of Arizona, Tucson, Arizona*
[m] *Institute of Atmospheric Physics, Chinese Academy of Sciences, Beijing, China*
[n] *Office of Hydrology, NOAA, Silver Spring, Maryland*
[o] *Meteorology Department, Reading University, Reading, United Kingdom*
[p] *Institute of Water Problems, Moscow, Russia*
[q] *Lawrence Berkeley National Laboratory, Berkeley, California*
[r] *Division of Atmospheric Research, CSIRO, Aspendale, Australia*
[s] *Institute of Geography, Moscow, Russia*
[t] *Climate Research Branch, Meteorological Service of Canada, Downsview, Ontario, Canada*
[u] *Mesoscale Dynamics and Precipitation Branch, NASA Goddard Space Flight Center, Greenbelt, Maryland*
[v] *Department of Geography, University of California, Los Angeles, Los Angeles, California*

(Manuscript received 25 February 2000, in final form 9 August 2000)

ABSTRACT

Twenty-one land surface schemes (LSSs) performed simulations forced by 18 yr of observed meteorological data from a grassland catchment at Valdai, Russia, as part of the Project for the Intercomparison of Land-Surface Parameterization Schemes (PILPS) Phase 2(d). In this paper the authors examine the simulation of snow. In comparison with observations, the models are able to capture the broad features of the snow regime on both an intra- and interannual basis. However, weaknesses in the simulations exist, and early season ablation events are a significant source of model scatter. Over the 18-yr simulation, systematic differences between the models' snow simulations are evident and reveal specific aspects of snow model parameterization and design as being responsible. Vapor exchange at the snow surface varies widely among the models, ranging from a large net loss to a small net source for the snow season. Snow albedo, fractional snow cover, and their interplay have a large effect on energy available for ablation, with differences among models most evident at low snow depths. The incorporation of the snowpack within an LSS structure affects the method by which snow accesses, as well as utilizes, available energy for ablation. The sensitivity of some models to longwave radiation, the dominant winter radiative flux, is partly due to a stability-induced feedback and the differing abilities of models to exchange turbulent energy with the atmosphere. Results presented in this paper suggest where weaknesses in macroscale snow modeling lie and where both theoretical and observational work should be focused to address these weaknesses.

1. Introduction

The impact of snow cover on climate at all spatial scales can be significant (Kukla 1981). Snow can cover over half of the Northern Hemisphere land surface during winter (Robinson et al. 1993), and, at a given point, snow cover can have a longevity varying from permanent to less than a few days. Most notable among the many properties of snow with respect to climate are its high albedo, low thermal conductivity and roughness length, and ability to store water within the hydrological cycle.

An analysis of observational data has indicated that the extent of snow cover can influence surface temper-

Corresponding author address: Andrew G. Slater, Campus Box 216, CIRES, University of Colorado, Boulder, CO 80309-0216.
E-mail: aslater@cires.colorado.edu

TABLE 1. List of acronym definitions for models to which this paper refers. For primary reference for each model, see Table 2.

Acronym	Model name
AMBETI	Agrarmeteorologisches Modell zur Berechnung von Evaporation, Transpiration und Interzeption
BASE	Best Approximation of Surface Exchanges
BATS	Biosphere–Atmosphere Transfer Scheme
BUCKET	Bucket
CLASS	Canadian Land Surface Scheme
CROCUS	—
CSIRO	Commonwealth Scientific and Industrial Research Organisation
IAP94	Institute of Atmospheric Physics Land Surface
ISBA	Interactions between Soil, Biosphere, and Atmosphere
MAPS	Mesoscale Analysis and Prediction System
MOSES	U.K. Meteorological Office Surface Exchange Scheme
NCEP	National Centers for Environmental Prediction
PLACE	Parameterization for Land–Atmosphere–Cloud Exchange
SECHIBA	Schématisation des Echanges Hydriques à l'Interface entre la Biosphère et l'Atmosphère
SLAM	Simple Land–Atmosphere Mosaic
SPS	Soil Plant Snow
SPONSOR	Semi-Distributed Parameterization Scheme of Orography-Induced Hydrology
SSiB	Simplified Simple Biosphere
SWAP	Soil Water–Atmosphere–Plants
UGAMP	U.K. Universities Global Atmospheric Modelling Programme
UKMO	United Kingdom Meteorological Office

atures during or after its existence (Dewey 1977; Robock 1983; Groisman et al. 1994) as well as alter circulation patterns (Lamb 1955; Leathers and Robinson 1993) and precipitation regimes (Namias 1985). Eurasian snow cover is of special relevance to the Asian monsoon, where there is both observed and modeled evidence that high winter/spring snow covers result in weaker monsoon precipitation (Vernekar et al. 1995).

In terms of modeling efforts, Yeh et al. (1983) suggested a strong climatic response to alterations in the snow regime. In contrast, however, Cohen and Rind (1991) note that climate response may be limited by negative feedbacks. These differing views are consistent with the results obtained by Cess et al. (1991) and Randall et al. (1994), in which the radiative response to snow cover of numerous general circulation models (GCMs) varied from a strong positive to weak negative feedback. Foster et al. (1996) undertook a comparison of the snow water equivalent produced by seven GCMs that showed some consistency between them but also a wide variety in the magnitude and temporal distribution within transitional seasons. Differences in this case were mostly attributed to inaccurate precipitation and temperature field simulations by respective GCMs. However, these fields are affected by feedbacks from the land surface and, for most models, reference was made to some deficiency of the snow submodel. Clearly, to improve the predictive ability of the global or a regional climate, confidence in the simulation of snow is necessary.

The development and validation of snow submodels for use in climate models has been undertaken by many groups (e.g., Loth et al. 1993; Lynch-Steiglitz 1994; Douville et al. 1995; Yang et al. 1997; Slater et al. 1998; Essery et al. 1999). These studies have shown how model specific parameterizations have contributed to simulation improvement or given explanations of results. Since 1992, the Project for the Intercomparison of Land-Surface Parameterization Schemes (PILPS) (Henderson-Sellers et al. 1995) has been systematically intercomparing the performance of land surface schemes (LSSs), but previous PILPS studies have not focused on the modeling of snow. Phase 2(d) of PILPS used data from Valdai, in the former Soviet Union (see section 2), to perform a suite of simulations. The aim of this paper is to investigate specifically how snow processes are represented within LSSs and to attempt to determine the reason for any scatter among the models, via systematic intercomparison [for an overview of all results from PILPS 2(d), see Schlosser et al. (2000)]. In the remainder of this paper we will briefly discuss the data and experimental design (section 2), validate the models against observations and compare them with each other (section 3), examine areas responsible for differences in results (section 4), investigate sensitivity to longwave radiation (section 5), and conclude (section 6).

2. Data and methods

A full description of data and experimental design for PILPS Phase 2(d) is given in Schlosser et al. (2000), thus only a brief summary will be given here. Twenty-one LSSs (Tables 1 and 2) were forced with 18 yr of observed meteorological data (1966–83) from a grassland catchment at the Valdai water-balance station (57°58′N, 33°14′E; Fedorov 1977). Vinnikov et al. (1996) and Schlosser et al. (1997) discuss the data in detail. A typical annual maximum snow water equivalent (SWE) value ranges from 120 to 170 mm, and January temperatures average about −12°C but can drop as low as −25°C. Snowfall typically begins in late October or November, and the snowpack can persist until

early May. One source of uncertainty in the SWE data lies in the fact that the snowfall rate provided as input to the LSSs may have been overestimated. A study carried out by Yang et al. (1996) suggests that, in comparison to a standard snow precipitation gauge, the Valdai system is largely free of the common problem of wind-induced gauge undercatch, but, under specific blowing snow conditions, it may have been subject to overcatch. Thus, the LSS would tend to overestimate the amount of snow on the ground in comparison with measurements. In the case of several LSSs, this phenomenon appears to be evident in some years (e.g., 1980/81 in Fig. 1). Measuring snow precipitation is not a trivial exercise, and the data used here are of suitable quality for our purposes because potential biases are known. As with any model validation study, however, care must be taken in interpreting or extrapolating from some results.

Downward longwave radiation (LWD) was not available from the observed data and, following the approach of previous studies (Yang et al. 1997; Slater et al. 1998), was determined via two empirical methods to test the sensitivity of LSS to LWD. The ''control'' simulation (CTRL) followed Idso (1981), and Brutsaert (1975) was used as a comparison in the lower longwave radiative forcing simulation (LNGW). Models used either 30- or 5-min time steps depending upon individual requirements. Equilibrium conditions and initialization of the experiment tend to have little bearing on snow simulation after the first season, so they are not discussed further here (see Schlosser et al. 2000).

Models defined precipitation to fall as snow when the air temperature was 0°C or below. Snow albedo was given a maximum (fresh snow) value of 0.85 for the visible and 0.65 for the near infrared, but again models were asked to use their own snow albedo schemes for the purposes of changing albedo as the snow aged and melted. Albedo of the underlying surface was specified across all models as 0.23. No specification was made for the fractional extent of snow cover of the ground and vegetation masking, though some models (e.g., IAP94; all model acronym definitions may be found in Table 1) maintained a predetermined snow-free fraction. The roughness length of snow was specified as 0.0024 m. Parameters concerning soil hydrology and vegetation were specified as consistently as possible across all models (see Schlosser et al. 2000).

This paper evaluates the models' simulations of SWE, which was determined using coring measurement data from a maximum of 44 snow courses throughout the catchment, though not all were used all the time. Measurements were made at uneven intervals. Over the duration of the snowpack, some seasons had as few as 6 measurements and others had up to 17.

3. Results

a. Validation

In comparison with observations, models are able to capture the broad patterns of snow accumulation and ablation (Fig. 1). However, in some years (e.g., 1967/68 and 1968/69) there is a consistent bias in which no or few models simulate excess SWE and most simulate too little SWE. In contrast, other years (e.g., 1970/71 and 1982/83) most models simulate excess SWE, with some models simulating 2 times as much SWE as observed. Some of the bias within a year may be due to the specification of the rain/snow criterion being different from observations or a problem with the forcing, such as overcatch (see section 2).

One area where models are consistently different from observations is their tendency to underestimate the extent of midseason ablation (e.g., the winters of 1970/71 and 1973/74, Fig. 1). Many models cease net accumulation during these periods, but they are generally unable to match observed ablation. The inability of models to simulate midseason ablation properly has previously been noted by Douville et al. (1995), Yang et al. (1997), and Slater et al. (1998), but the underlying reasons have yet to be identified. This consistent misrepresentation is one area where attention could be focused to improve the simulation of snow processes in land surface models.

The ability of models to simulate the observed snow cover does not appear to be related to the amount of snow that falls. Prima facie, low-accumulation years (e.g., 1971/72) are simulated with skill equal to high-accumulation years (e.g., 1980/81), and it appears that the number and strength of ablation events (periods of short rapid ablation) within a season are a greater determinant of the extent of scatter. Clearly, although there is scatter among the models, there is some skill in all models, independent of complexity, to simulate the seasonal cycle in SWE and interannual differences in SWE.

b. Intercomparison

In comparison with each other, there is a relative coherence among the models in terms of the maximum SWE or length of snow season simulated. For example, MOSES and SECHIBA tend to display a lower SWE than the other models whereas CLASS and SPS tend to produce longer seasons [Fig. 1 and Fig. 7 of Schlosser et al. (2000)]. Across all the models, the December–February (DJF) range is an average of 50 mm in SWE, with a standard deviation of 12 mm. There is an average of a 40-day difference each year between the first model to melt all simulated snow and the last.

Early-season ablation appears to be a major source of divergence among the models, but unfortunately few observations span these events. It is therefore unclear which models were able correctly to capture snow processes at this time, which makes validation difficult (an example of this model divergence is seen in the winters of 1972/73, 1976/77, and 1980/81). The intermodel scatter of SWE increased from 10 to 40 mm over several days in early December 1972, and was caused by models ablating the snow cover at very different rates. The like-

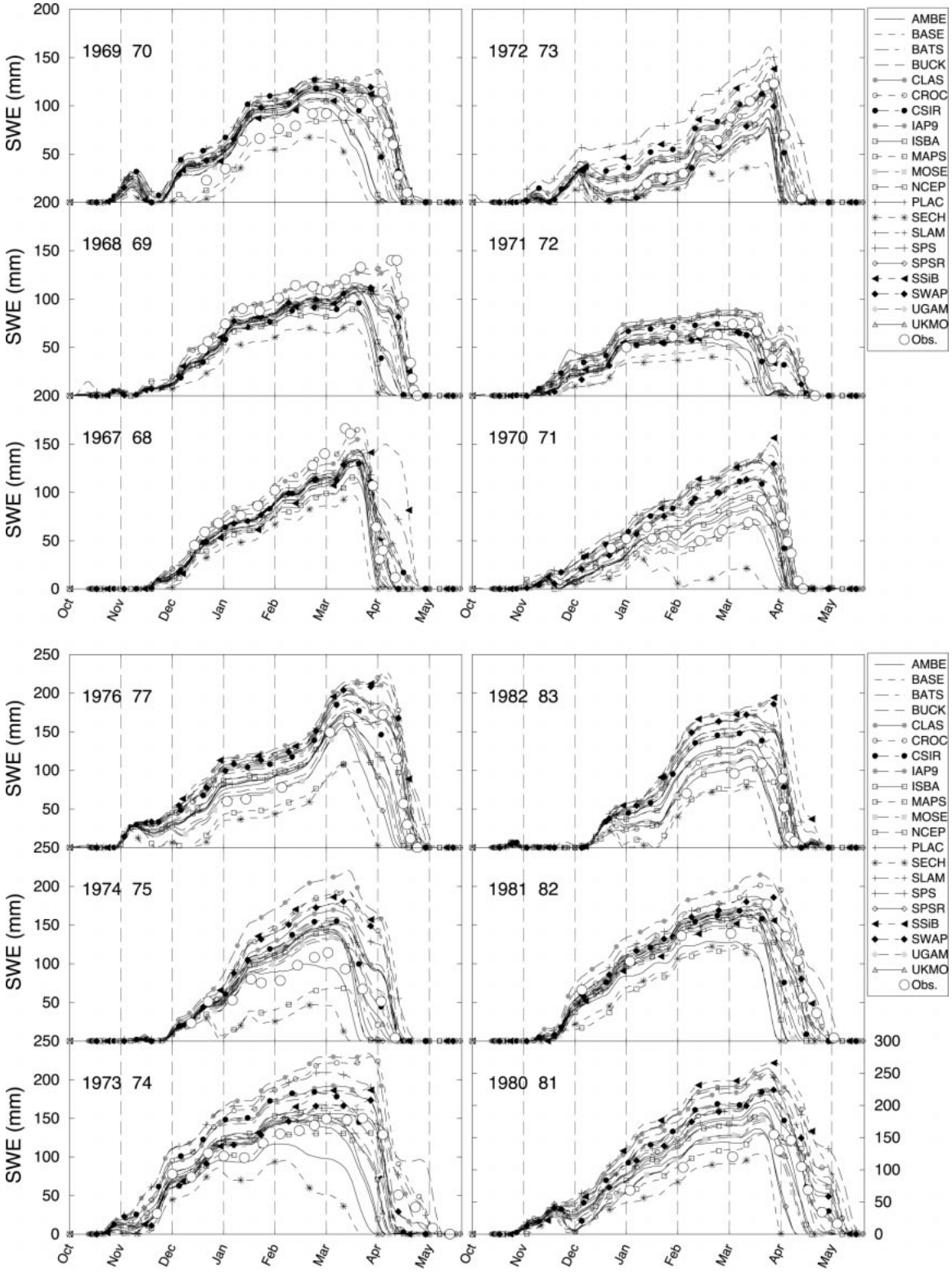

FIG. 1. Daily averaged SWE, (mm) as a time series with a 7-day running mean shown for the various winters mentioned. Observations are shown as the large open circles.

TABLE 2. Key features of snow submodels in PILPS 2(d). Items marked with * indicate standard model setup, not as was used in PILPS 2(d). References are supplied for specific methods if they do not fit predefined categories. Albedo: the main control upon the value of snow albedo is listed. Fractional cover: asymptotic refers to a function such as $F_{sno} = S_{depth}/(S_{depth} + CZ_{0,veg})$, where S_{depth} is the snow depth, C is a constant, and $Z_{0,veg}$ is the roughness of vegetation. Density: F refers to a fixed density, AGE to a time function, and TMCV to a thermodynamic and compactive viscosity method.

Model	Albedo	Fractional cover	Density (ρ)	ρ range (kg m^{-3})	Thermal conductivity (W m^{-1} K^{-1})	Reference
AMBETI	Density	100%	AGE, linear	100–500	$K_{tn} = 8.5 \times 10^{-4}\,\rho - (5.0 \times 10^{-3})$	Braden (1995)
BASE	Temperature	Asymptotic	TMCV, Kojima (1967)	100–450	$K_{tn} = 2.805 \times 10^{-6}\,\rho^2$	Desborough and Pitman (1998), Slater et al. (1998)
BATS	Age	Asymptotic	AGE, Yang et al. (1997)	100–400	$K_{tn} = 2.93 \times 10^{-6}\,\rho^2$	Dickinson et al. (1993), Yang et al. (1997)
BUCKET	Fixed	–	–	–	–	Robock et al. (1995)
CLASS	Age	Linear below 10 cm	AGE, exponential, Verseghy (1991)	100–300	$K_{tn} = 2.576 \times 10^{-6}\,\rho^2 + (7.4 \times 10^{-2})$	Verseghy (1991)
CROCUS	Age, grain size, and type	Asymptotic	TMCV, Navarre (1975)	30–917	$K_{tn} = 2.22\,(r/1000)^{1.88}$ **	Brun et al. (1989, 1992)
CSIRO	Age	Asymptotic	TMCV, Kojima (1967)	100–350	$K_{tn} = 2.5 \times 10^{-6}\,\rho^2 + 2.0 \times 10^{-2}$	E. A. Kowalczyk (unpublished manuscript)
IAP94	Fixed* age (BATS)	Specified, asymptotic	TMCV, Anderson (1976)	100–500	$K_{tn} = 0.023 + (2.267 \times 10^{-5})(7.75\rho + 0.1105\rho^2)$	Dai and Zeng (1997)
ISBA	Age	Asymptotic	AGE, exponential, Verseghy (1991)	100–300	$K_{tn} = 2.22(\rho/1000)^{1.88}$	Douville et al. (1995), Noilhan and Mahfouf (1996)
MAPS	Fixed	100%	Fixed	400	$K_{tn} = 0.35$	Smirnova et al. (1997)
MOSES	Depth	100%	Fixed	250	$K_{tn} = 0.265$	Cox et al. (1999)
NCEP	Depth	Asymptotic	TMCV, Kojima (1967), Anderson (1976)	50–500	$K_{tn} = 10^{(-4.04 + 0.00225\rho)}$	Chen et al. (1996), Koren et al. (1999)
PLACE	Age	Linear to 50 mm SWE	TMCV, Anderson (1976)	50–550	$K_{tn} = 2.576 \times 10^{-6}\,\rho^2 + (7.4 \times 10^{-2})$	Wetzel and Boone (1995)
SECHIBA	Fixed	Asymptotic	Fixed	325	$K_{tn} = 0.30$	de Rosnay and Polcher (1999), Chalita and Le Treut (1994)
SLAM	Age	Asymptotic	TMCV, Kojima (1967)	100–450	$K_{tn} = 2.805 \times 10^{-6}\,\rho^2$	Desborough (1999)
SPS	Fixed	100%	–	–	–	Kim and Ek (1995)
SPONSOR	Depth	100%	Variable, Shmakin (1998)	100–500	$K_{tn} = 0.67\,(6 \times 10^{-12}\,\rho^4 + 0.0019\rho + 0.005)$	Shmakin (1998)
SSiB	Temperature	Linear	Fixed	200	No explicit snow thermal conductivity, same as top soil layer	Xue et al. (1991, 1996)
SWAP	Depth	100%	TMCV, Yoshida (1955)	200–320	$K_{tn} = 0.419\,(6 \times 10^{-12}\,\rho^4 + 0.0019\rho + 0.05)$	Gusev and Nasonova (1998)
UGAMP	Age	Linear below threshold 10 cm	Fixed	200	$K_{tn} = 0.107$	Gedney (1995)
UKMO	Depth	100%	Fixed	250	$K_{tn} = 0.265$	Warrilow and Buckley (1989)

** For small values of thermal conductivity in CROCUS, it depends on water vapor in the snow and snow density.

ly cause of the increased scatter is the thin snow cover in early winter, which has a greater sensitivity to forcing changes. Much of this high sensitivity results from differences in fractional cover, albedo, and thermal properties across the models that are greatest for thin snow cover (section 4). Furthermore, much of the initial difference among models is maintained during the course of the whole snow season as internal feedback mechanisms, such as the albedo/energy availability feedback, come into play. A similar explanation applies to end-of-season snowfall when fresh snow may melt if it falls onto bare ground but may extend the presence of snow if it falls onto an established snowpack (e.g., the springs of 1972 and 1974; see Fig. 1).

Although the models are able to capture the basic features of the SWE observations, there are considerable differences between their simulations. The importance of these early-season SWE differences is evidenced by their tendency to persist throughout the whole snow season. Most models are able to simulate a rapid final melt of their snowpacks, and it is likely that for this final melt the snowpacks have reached a ripe state and the springtime increase in energy available for melting leads to a rapid end. However, the date at which a snowpack ripens is a function of snowpack evolution during the earlier part of the season, and, as a result, the timing of spring melt varies across the models by about a month.

Given that, when compared with each other, the models tend to behave similarly from year to year in terms of both maximum SWE and snow season length, it is likely that there are systematic differences among the models; these differences are explored next.

4. Influences on snow water equivalent simulations

Because snowfall is prescribed, differences in the simulation of SWE are caused by ablation of snow through melting and evaporation and direct air–snow sublimation. LSSs melt snow when it contains too much energy to stay below 273 K, and we therefore need to investigate how land surface parameterization affects the temperature regime of the surface.

Three areas have been identified as being influential upon temperature and ablation of snow: 1) vapor exchange at the snow surface (section 4a); 2) the amount of energy incident on and available to the snow, which is primarily controlled by albedo and fractional cover (section 4b); and 3) the structure and thermal properties of the snow (section 4c). Because different implementations of these factors within the one LSS make it difficult to produce generalized rules relevant to all models, specific models are referred to where appropriate.

In the following sections we investigate various aspects of snow submodels and how they affect SWE. The implications with respect to the predictive ability of these models are also discussed.

a. Sublimation from the snow surface

With prescribed snowfall, the exchange of water vapor between snow and air is one of only two degrees of freedom in the snowpack moisture balance. Net snow sublimation varies considerably among the models (Fig. 2), with one model having net frozen condensation and others ablating up to 15% of total snowfall through evaporation. Evaporation occurs mainly at the beginning and end of the snow season when available energy is relatively high. However, many of the models simulate deposition onto the snowpack in the midwinter.

The CSIRO and BUCKET models stand out in spring as having very high evaporation, but during the midwinter period SECHIBA and ISBA show the highest evaporation rate. This result in part explains the high ablation rates shown by these two models. BATS and CROCUS, on the other hand, show the strongest instances of negative evaporation of all the models in the CTRL simulation.

A generalized description of evaporation from the snow surface (E_{snow}) can be given as

$$E_{\text{snow}} = \rho_a U_a C_w [e(T_s) - e_a]$$

(e.g., Anderson 1976), where $e(T_s)$ is the saturation vapor pressure at the snow surface according to the Clausius–Clapeyron relation, e_a is the vapor pressure of the air, U_a is the wind speed, ρ_a is the density of air, C_w is the bulk transfer coefficient of water vapor, and all models follow an analogous formulation. Among the models, the main source of difference in evaporation from the snowpack will be either the vapor gradient $[e(T_s) - e_a]$ or the transfer coefficient C_w. Given that the vapor pressure of the air is supplied in the forcing data at a specified height, the vapor gradient will be determined by the snow surface temperature, and, as Fig. 3a shows, the surface radiating temperature in mid-winter (which acts as a surrogate for the snow temperature as snow cover is at or close to 100%) can differ by over 10 K across all the models. Simple regression analysis suggests that there is not a clear and direct relationship between surface temperature and evaporation rate, and it is likely that the determination of the aerodynamic transfer coefficients has an important role in explaining the scatter among models. Roughness lengths and wind speeds were prescribed to be equal across the models; thus differences in transfer coefficients for sensible and latent heat are likely to be caused by differences in the parameterized dependence of the coefficients on the land–air temperature gradients. Formulations such as that of Louis (1979) are often used in LSSs to determine transfer coefficients for the surface layer, but the specific implementations can differ (e.g., Pan et al. 1994; Abdella and McFarlane 1996; Viterbo et al. 1999). In very stable cases, models may become uncoupled from the atmosphere, and, as Beljaars and Holtslag (1991) indicated, this problem may have been neglected by modelers (section 5). A further consideration is that blowing-

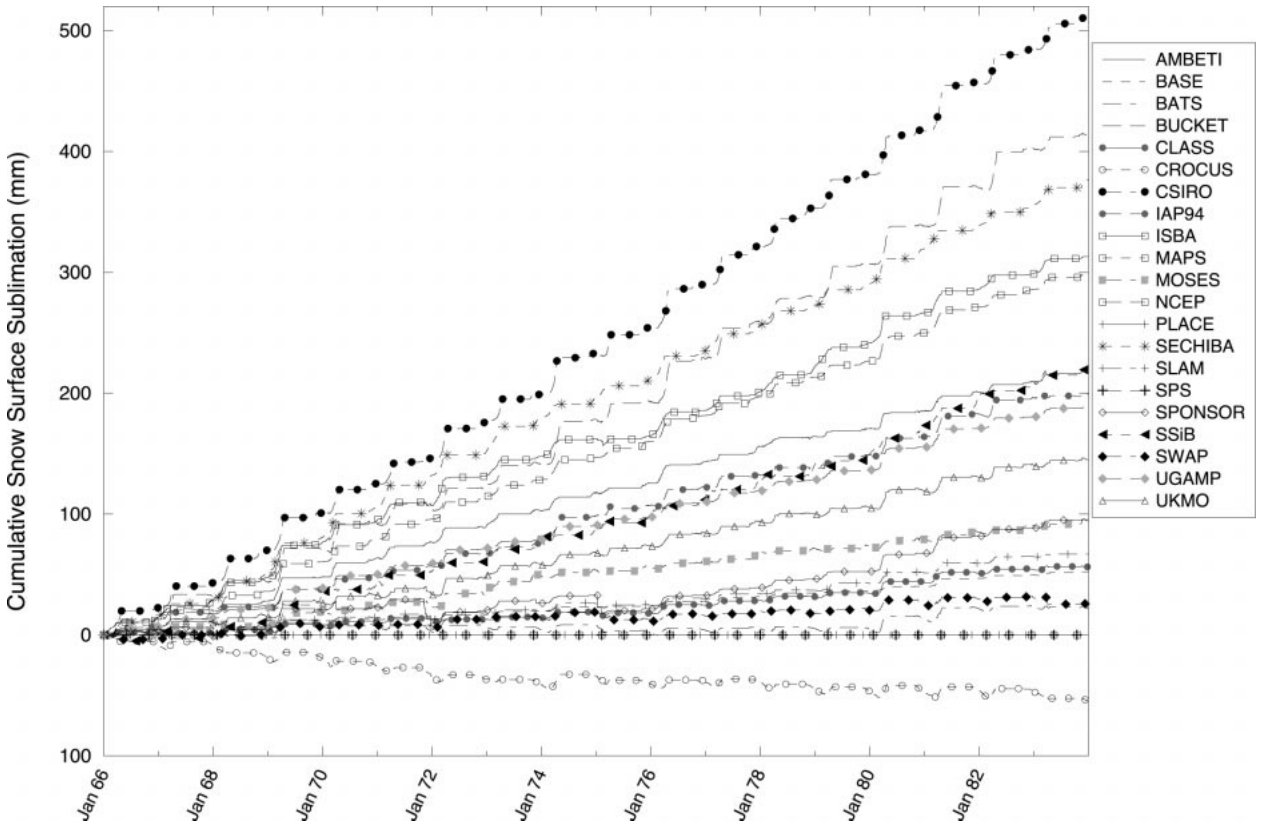

FIG. 2. The cumulative evaporation (mm) from snow over the 18 yr of the CTRL simulation. (PLACE did not report this variable.)

snow parameterizations are not included in LSSs for purposes of either snow redistribution and sublimation, yet in some locations can be significant ablation processes (Pomeroy et al. 1998; Pomeroy and Essery 1999). An improved understanding of the snow evaporation process through observational work should aid the representation of snow in land surface models since there are few data available.

b. Albedo

Absorbed solar radiation differences make a large contribution to energy-input differences, especially during the melt period. In February and early March, there is a range of 25 W m^{-2} in absorbed solar radiation across the models, and it increases to over 50 W m^{-2} from late March and into April. With incident shortwave prescribed, net shortwave varies between models as a result of snow albedo and fractional cover differences. Differences between the models' relationship of terrestrial (or grid-box average) albedo to SWE are shown in Fig. 4. In most models, terrestrial albedo, which is a function of both snow albedo and the fractional area it covers, rapidly increases as SWE increases within the range of 0–50 mm; however, the rate at which it increases varies among the models. For example, PLACE requires 50 mm of SWE to reach its maximum albedo, BUCKET needs 20 mm, and SWAP needs only 10 mm. The rate at which maximum albedo is reached reflects the rate at which models assume snow to cover bare ground and mask the canopy. As noted above, the periods in which SWE is low produce the greatest difference among the models. Over midwinter (DJF), a time series of albedo (not shown) indicates that the modeled albedo is mostly confined to a range of 0.70–0.75 as the snow ages or varies in temperature. However, at this time the amount of incoming solar radiation is relatively small, again suggesting that the period primarily responsible for scatter in SWE is early in the snow season.

Figure 4 also shows that two models show a distinctly different albedo regime. CLASS maintains a low terrestrial albedo until a sufficient depth of snow has accumulated to mask the vegetation. One consequence of this is that the longevity of the snow cover can be high even while the terrestrial albedo remains low. AMBETI has a minimum terrestrial albedo of 0.35 in the presence of snow, and this varies in a linear fashion; thus, a large value of SWE is required before terrestrial albedo approaches the maximum of 0.75. Not surprisingly, AMBETI is also a model that melts snow cover relatively fast.

Yang et al. (1997) investigated the issue of fractional snow cover with the BATS model and showed a variety of methods used to calculate this quantity. They showed

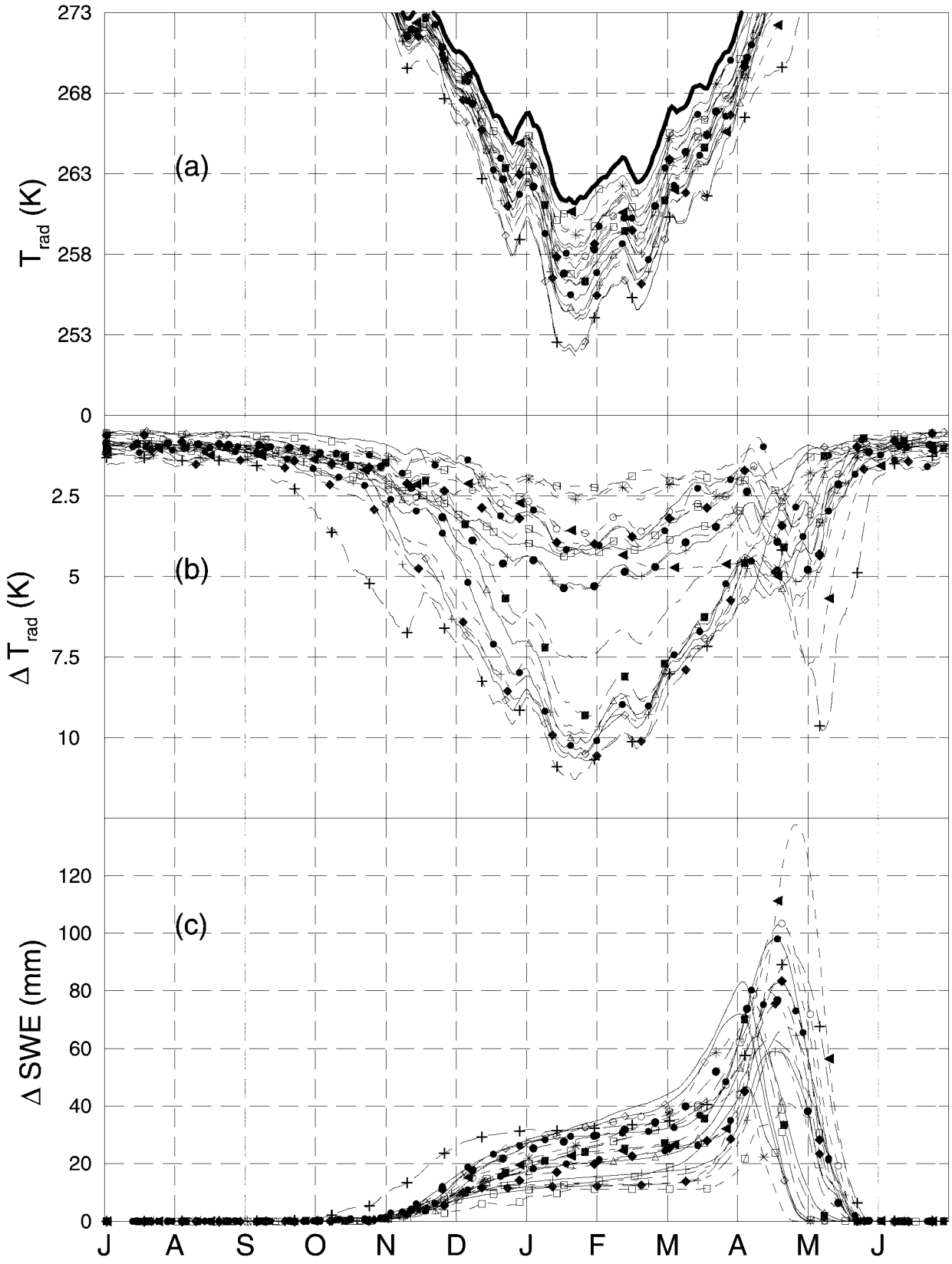
(a)
(b)
(c)
T_{rad} (K)
ΔT_{rad} (K)
Δ SWE (mm)
273
268
263
258
253
0
2.5
5
7.5
10
120
100
80
60
40
20
0
J
A
S
O
N
D
J
F
M
A
M
J

that increasing the fractional cover under an identical forcing has the effect of increasing the longevity and mass of snow at both the beginning and end of the season, and this illustrates the internal feedback that will occur within most models. In this respect SPS, which instantly has a fractional cover of 1.0 and a snow albedo of 0.75, is aided in maintaining a higher SWE in the early part of the snow season because energy flux into the surface is lower than that of the other models.

Few studies have looked into the macroscale distribution of snow cover, and few observations are available for a range of time- and space scales as required by climate models. Much of the lack of observed fractional snow cover stems from the definition of this term, with most models defining it as the proportion of the grid square that the atmosphere actually ''sees'' as being covered with snow, and then using this for albedo calculations (although it can be used in other calculations such as flux aggregation). Regardless of how fractional cover is parameterized, it can have a different effect depending upon the structure of the model. The impact of applying similar parameterizations in differing model structures has been noted previously in PILPS (Desborough 1997) and other experiments (Smirnova et al. 1997). A fractional snow cover of 10% in a model with an explicit snow layer [i.e., snow layer(s) modeled separately from the soil, with their own temperature and hydrological conditions; see Fig. 5] will have a different impact upon the simulation of snow in comparison with a fractional cover of 10% in a model with a composite snowpack. In the former case, snow temperature can stay low because of a high albedo and low energy diffusion across the snow–soil interface. In the latter case, if the snow and soil layer are considered to be homogenous horizontally (Fig. 5), the lower albedo of the soil has a direct influence upon the energy available to the snow temperature calculation. In addition, fractional cover will determine the influence of longwave radiation (which is the dominant radiative flux over midwinter). To account for snow extent on the ground, Sellers et al. (1996) used an algorithm based on satellite-derived data from Chang et al. (1990), but the protrusion of vegetation above the ground cover still remains a problem in forest areas. With respect to GCMs, Tao et al. (1996), in an analysis of the Atmospheric Model Intercomparison Project (Gates et al. 1992) models, indicated that perhaps the cold bias found in winter over the continents (particularly Eurasia) may be attributable to the lack of an appropriate snow cover fraction because of vegetation protrusion.

The principles of snow albedo at the small scale have been well established (e.g., Wiscombe and Warren 1980; Warren and Wiscombe 1980) with spectral dependence, grain size and type, and contamination being important factors. A variety of methods for parameterizing snow albedo within an LSS have been used, ranging from fixed values (e.g., SPS, MAPS, IAP94) to calculations making allowance for temperature (e.g., BASE, LSM; Bonan 1996), age (e.g., CLASS, ISBA, UGAMP, SLAM), extinction coefficients (AMBETI, CLASS), and solar zenith angle (BATS), either singularly or in combination. Given that bare ground and vegetation albedo were specified at 0.23 in these experiments and that most models will assume that the grid box is fully covered with snow cover when SWE is above 150 mm, Fig. 4 shows that for the more complex models there is a degree of spread in determining actual snow albedo. For example, BASE, MOSES, SLAM, and UKMO have a range of 0.75–0.58 but CROCUS and BATS occasionally exceed 0.80. However, snow albedo alone cannot explain all the scatter in SWE, because it must be considered in combination with fractional cover to determine the amount of solar radiation absorbed by the whole surface. Then, one needs to consider how that energy is distributed (section 4c), the effective albedo of the surface considered within the calculation of the temperature assigned to snow, and how these factors will vary depending on the structure of the model.

Issues regarding spatial heterogeneity have been well documented elsewhere (e.g., Giorgi and Avissar 1997), but specific to snow is the way it is distributed within the fraction of a grid square covered by snow (either patchy or uniform). This issue is not explicitly considered within LSSs, because it is considered to be of lesser importance, but local advection does contribute to snowmelt (Liston 1995; Essery 1997; Neumann and Marsh 1998). In addition, fractional cover becomes more complex if a forested grid square is modeled, because a bulk value of fractional snow cover for albedo purposes may be incongruent to a value needed for thermal or evaporative purposes, especially in an implicit snow scheme (Fig. 5) that cannot separately consider snow cover of bare ground and masking of vegetation (Essery 1998). Snow cover in boreal forests has recently received attention because of campaigns such as the Boreal Ecosystem–Atmosphere Study (Sellers et al. 1997), and noted improvements have been made to global forecast models (e.g., Viterbo and Betts 1999). The use of remotely sensed imagery for determining characteristic distributions has been suggested as a solution (Liston 1999) and offers potential for certain applications. Satellite-based products give the best hope of capturing global-scale subgrid snow distributions, but sensors to date have not been able to provide snow-depth and

←

FIG. 3. Daily average values, averaged over the 18 yr with a 7-day running mean, of the following variables: (a) surface radiating temperature (K) for the CTRL run, in which the thick black line is the point of neutral stability, i.e., air temperature; (b) The LNGW simulation less the CTRL simulation for surface radiating temperature (K); and (c) SWE for the LNGW simulation less the CTRL simulation.

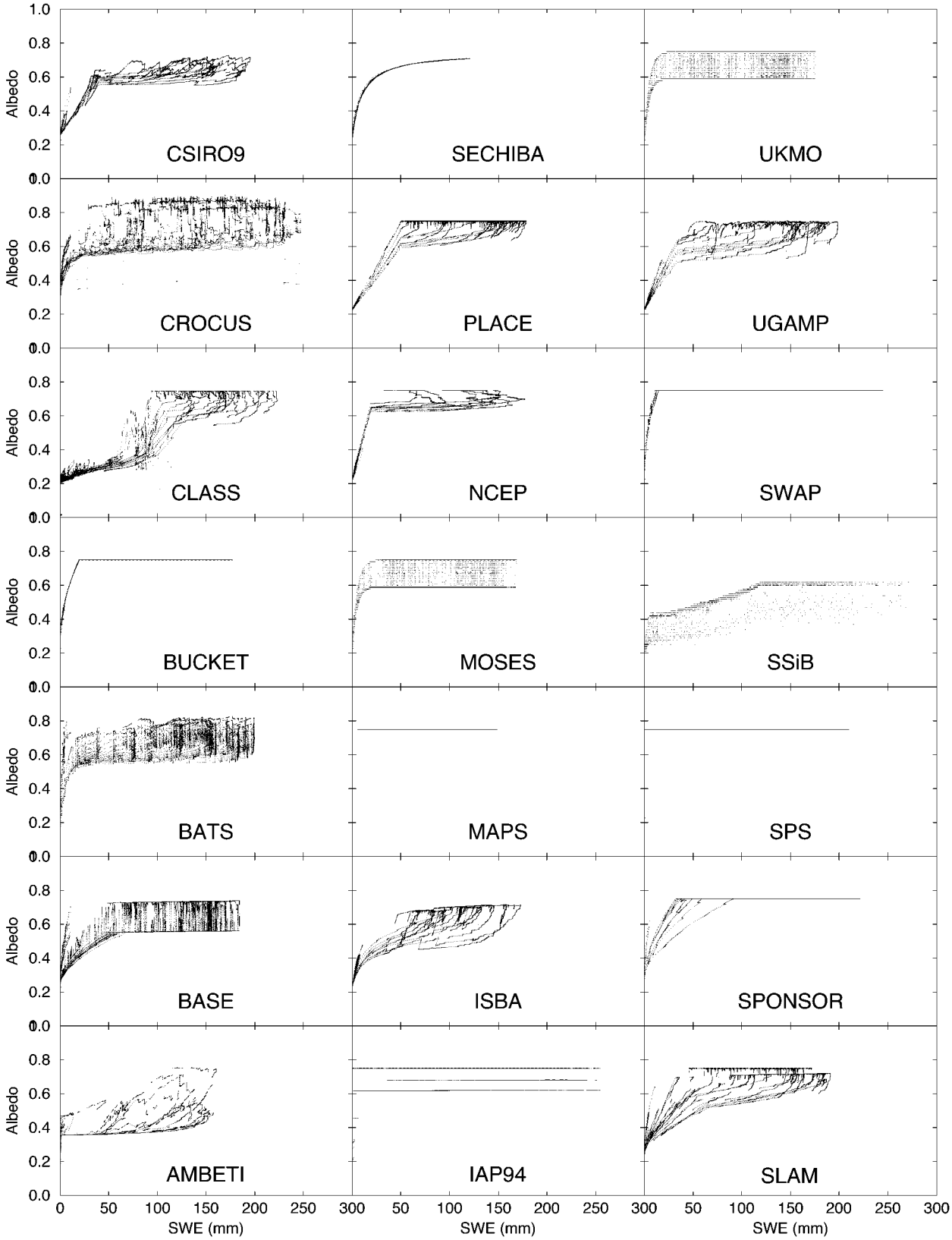

FIG. 4. Time step values of terrestrial albedo plotted against SWE (mm) for each of the 21 models.

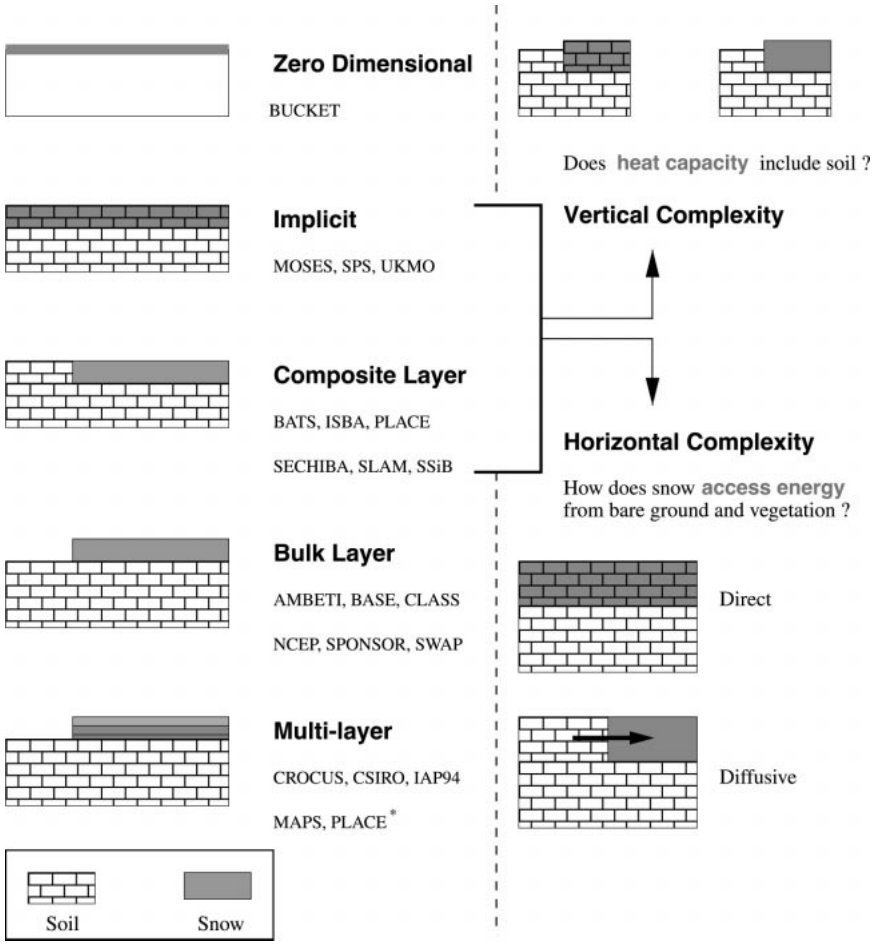

FIG. 5. A classification of model structures with respect to the snow temperature and absorption of incoming radiation. A zero-dimensional scheme computes temperature via an energy balance over a uniform surface. An implicit scheme assumes an even cover of snow upon the grid square and makes compensations to its soil and vegetation surface properties to allow for the mass of snow. A composite layer model will track various quantities for its snow cover, such as fractional cover, but snow temperature is equal to that of the first soil layer, which may eventually become 100% snow. Implicit and composite schemes can then include variations in horizontal and/or vertical complexity. Bulk layer and multilayer models include a one-layer or multiple-layer snowpack sitting above the soil system, respectively. Note that the multilayer schemes move in and out of the other structures in low-snow conditions (see Section 4c).

snow-coverage data with the accuracy desired by the land surface community, especially in areas with forest canopies (e.g., Tait 1998).

c. Model structure and thermal properties of the snow

The energy input to the snow is the difference in radiative fluxes minus sensible and latent heat and the partitioning of energy across components of the surface such as bare soil, vegetation, and snow. The structure of the snow model (Fig. 5) plays an important role in determining energy availability as well as determining how that energy is used. The quantity of moisture deemed to be snow can be modeled as an explicit part of the LSS, and a set of separate quantities, such as albedo or heat fluxes, are calculated for it, with the resultant grid box quantities being an aggregate of the snow portion combined with other sections (e.g., canopy or bare soil). An alternative structure is to have an implicit snowpack, and what could be termed a set of allowances is made to the soil/canopy model. With the former method, all interactions with the snowpack are concentrated into the fraction of the grid that is deemed to be covered with snow, whereas the latter method assumes a more even interaction with a grid box that is an average of its components (Hess and McAvaney 1998). There is a graduation in the extent of explicit versus implicit snow submodel. For example, CROCUS is a multilayer model that operates as a separate layer above the soil layers within a fractional cover, CLASS has similar constraints but is a bulk-layer model; BATS

maintains a gridbox fraction in which to operate its snow model, but thermally the snow and first soil layer function as a singe unit; UKMO is an implicit scheme; and BUCKET is effectively a zero-dimensional model in this respect.

The influence of surface structure is evident in the simulation of SWE. For example, SECHIBA maintains a constant snow albedo of 0.75 and varies the fractional cover of snow (Fig. 4); however, because it is an implicit snow scheme, the temperature of the snow is the same as that of the first soil layer, and thus lower fractional cover results in greater absorption and availability of incoming energy to the snow. This result is in part reflected in the fact that SECHIBA consistently has the lowest SWE value. [Note that this version of SECHIBA does not include developments by Chalita and LeTruet (1994) for the Laboratoire de Meteorologie Dynamique GCM, such as vegetation masking by snow and an age-based snow albedo.] If the snowpack is explicit and displays a low fractional cover, the result is merely that soil–snow or atmosphere–snow interactions are concentrated in a small fraction of the grid. In an explicit scheme, snow temperature is modeled on its own. Thus, if snow albedo is high (yet terrestrial albedo can be low) snow absorbs little energy and can maintain a cold temperature leading to slow ablation. Such a situation is evident in the CLASS model, which consistently holds its snow cover longer and has a slower ablation rate than other models at the end of the season, yet it is not necessarily the model with the highest SWE at midseason. This result is well illustrated at the end of the 1970/71 and 1971/72 seasons. This tendency on the part of CLASS has been noted in other modeling studies (Pomeroy et al. 1998) and is caused by the fact that, as the modeled fractional area decreases, the snow depth is kept at 0.10; that is, the snowpack begins to melt from the sides rather than from the top. Such an approach may lead to unduly long persistence of the snowpack in some cases (although with vanishingly small values of SWE). With such a low fractional cover, the snowpack receives only a small amount of incoming solar radiation, and, during periods of low SWE, CLASS can maintain a columnlike snowpack as compared with the thin ''pancake'' snowpacks that are more common in the other models. The development of an improved characterization of fractional cover and snow depth is the subject of current research.

The effect of differences in the underlying snow/soil model philosophy was demonstrated by Lynch et al. (1998). They showed that, under the composite snow structures in BATS and LSM, the soil temperature calculation method and the way in which snow accessed that energy were important factors in explaining the difference between the models. Yang et al. (1999a), in a simulation using the Valdai data, suggest that the use of a bulk-layer diffusive/iterative energy balance model in LSM may not be suitable for calculation of snow surface temperature as compared with the force–restore (FR) method of BATS. However, Tilley and Lynch (1998) indicate that the FR method may not be appropriate for simulation of soil temperature and hydrological conditions in permafrost locations, because it can become too cold and unresponsive. Such differences can be resolved by realizing that if heat conduction into the snow for a single bulk layer follows a diffusion equation, it can only be made close to reality for one timescale. A bulk layer effectively filters out fast time responses but is suitable for long-timescale seasonal variations of heat flux. The latter are critical for getting soil temperatures right; thus the bulk-layer model should be an appropriate choice for a one-parameter snow model intended to get soil temperature correct. The FR method, on the other hand, by modeling diurnal diffusion, allows a good estimation of the temperature of the top snow surface. On longer timescales, the diffusive fluxes are increasingly small in comparison with other surface fluxes and therefore are less important to include for snow surface temperature calculation. Hence the FR can be expected to simulate daytime temperature peaks, as driven by solar heating and not to be a source of serious error for longer period variations. For a one-parameter model in which snow melting is largely controlled by daytime solar heating, elevating the surface of the snowpack to above freezing, FR is an appropriate choice if surface temperatures and snow melting are the objective. However, it inevitably conducts heat from the underlying soil orders-of-magnitude faster than would be appropriate for a thick layer of snow, so that the soil temperature follows the diurnal average surface temperature, whereas observation might show the soil temperature has not dropped much below freezing (e.g., Tilley and Lynch 1998). Thus, to simulate both snow surface temperature and temperature at the snow–soil interface (e.g., for modeling carbon fluxes; Schimel et al. 1994), a multilayer model that has been validated to work as well as FR for surface temperatures over the diurnal cycle, and to give temperatures at the soil interface as well as the bulk layer model does, is required (which is the current trend among model groups).

The temperature of the snow within a model is the determinant of its ablation characteristics. The effective heat capacity of the snow will depend upon the thermal properties and the structure of the model. The limits on heat capacity of snow vary widely across models. For example, LSM uses a bulk heat capacity of the whole snow slab, with an imposed upper limit of a 1-m slab with density of 250 kg m^{-3}, which will be invoked at locations such as Antarctica and the southeastern corner of Alaska, where snow depths are typically high (cf. Foster et al. 1996). Conversely, the Simple Biosphere model, version 2, (Sellers et al. 1996) uses an effective heat capacity for snow that is limited to 0.05 m of SWE so as to allow for diurnal variation of surface temperature. E. A. Kowalczyk (1999, unpublished manuscript) notes the impact of altering the heat capacity of modeled snow by comparing a one-layer to a three-layer scheme

utilizing the same physics. Because of the higher heat capacity of the single-layer model, snowmelt is delayed when compared with the three-layer models, and the impact on subsurface hydrological behavior is also evident. Sud and Moko (1999) incorporated a bulk-layer snow model in SSiB to overcome problems such as a lack of response to forcing perturbations and a lagged melt (e.g., 1967/68; Fig. 1) in the old composite model. Their new model melts less in the early season but tends to ablate the snowpack at a more appropriate time. With respect to the influence of model structure on snow simulation, results presented here are consistent with those of Sud and Moko (1999) and Lynch et al. (1998).

Figure 5 shows that there are several ways in which the heat capacity of the snowpack can be calculated and linked to the soil structure of the model. The way in which energy is moved between the soil and snow varies depending upon whether a separate temperature is calculated for snow, whether diffusion processes need to be modeled, or whether the snow temperature is actually a composite of a snow/soil layer. Alternative schemes exist in which a model may move from one method of determining heat capacity to another depending on such factors as snow depth. For example, in PLACE, light snow is incorporated into the biomass layer of the soil grid, but as snow deepens the grid is moved up into the snowpack. This is done as a continuous function; thus a model layer can be all snow if the snowpack is deep enough, but in the transition period a layer can be a mix of soil and snow. New snow is transferred continuously from the biomass layer to the underlying soil grid; this transfer keeps the surface layer small, and therefore surface temperature can have large amplitudes (e.g., large nighttime cooling). Snowmelt is transferred back to the biomass layer, resulting in a relatively slow response in surface temperature as effective heat capacity of the surface layer is augmented. Additionally, conventional multilayer schemes use various values for dividing the snowpack; MAPS will accumulate a snow depth of 7.5 cm prior to becoming a two-layer scheme, whereas CSIRO requires 11 cm before becoming a three-layer scheme. Choice of appropriate discretization will depend on complexity of overall model physics and intended application.

The results from UKMO and MOSES provide a fine example of how underlying model structure and philosophy can produce simulation differences. Both models share most of the same parameterizations and are both implicit schemes (Fig. 5). However, UKMO uses a bulk temperature of surface snow/soil layer for turbulent flux calculations and does so before applying melt. MOSES uses a surface skin temperature and iterates the surface energy balance to be consistent with 0°C surface temperature when melting. Hence, turbulent fluxes make greater contributions to snowmelt, and MOSES tends to melt snow faster than UKMO does (Fig. 6). The use of a skin temperature should make the model more responsive to forcing (Viterbo and Belljaars 1995),

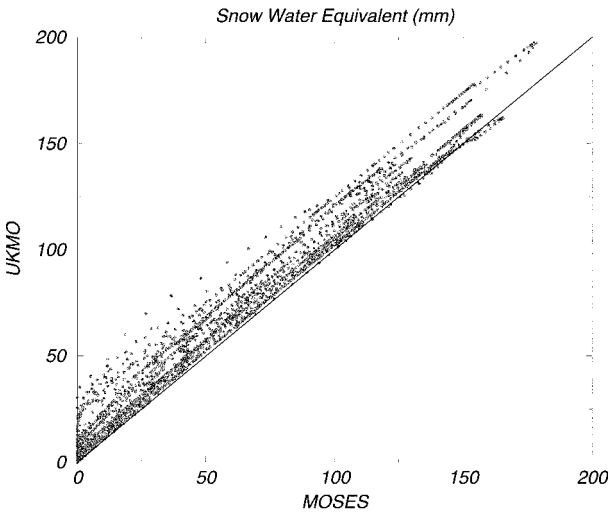

FIG. 6. Daily average SWE for UKMO vs MOSES for the full 18-yr simulation. Both models use the same parameterizations for thermal, radiative, and hydrologic properties of snow, but differ in temperature calculations and underlying soil models.

though in some situations it can overestimate the diurnal amplitude (Betts et al. 1997).

As mentioned in section 3, models have difficulty in ablating snow at midseason. Possible reasons for this difficulty may include that most LSSs use a bulk snowpack or snow/soil slab for the snow system. Thus this whole snow system has to reach 0°C before melting can take place. The effective heat capacity of this ''snow system'' can vary depending upon the model structure and factors such as the thickness of snow/soil layers (Fig. 5). The time step of the model can also have an influence. BUCKET has a flatter ablation curve than the rest of the models and is usually one of the last models to melt all of its snow. This result may be an artifact of the fact that this model does not explicitly resolve a diurnal cycle (cf. Manabe 1969); that is, although the daily averaged value of incoming energy is the same as for other schemes, the lack of warm periods during daytime, which perform ablation, is not equally compensated for by a warmer (though still below freezing) period at night. This fact in part explains why BUCKET extends its snow season beyond all other models for 1974.

LSSs that explicitly model snow density generally use it as a diagnostic variable for the calculation of other variables, such as depth (and hence fractional cover; section 4a) or thermal conductivity (Table 2). Many models assume density to be fixed, with the value usually between 100 and 350 kg m^{-3} (Table 2). However, as Sturm and Holmgren (1998) and Sturm et al. (1995) indicated, various snow ''types'' from differing geographical regions tend to group into density categories, but there does not appear to be a universally applicable global value. An alternative to using a constant value is to determine snowpack density based upon a time

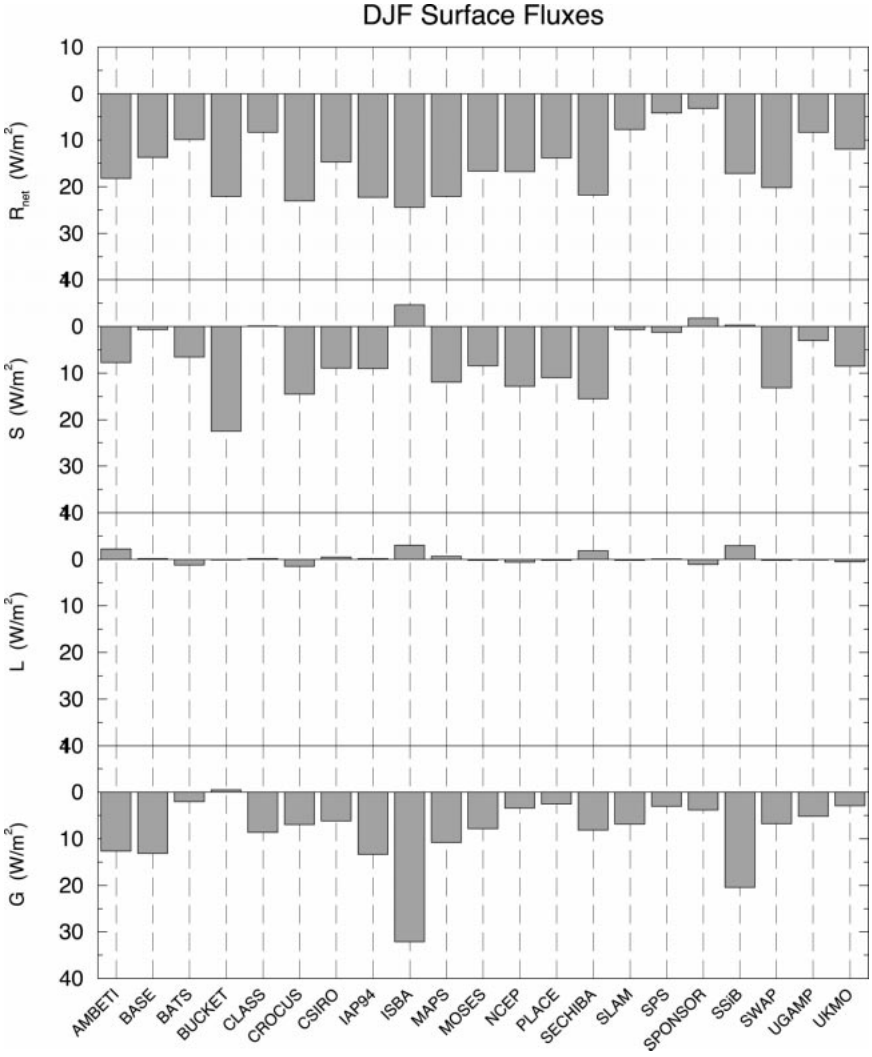

FIG. 7. Average values determined over the Dec–Feb period for a) net radiation (R_{net}), sensible heat (S), latent heat (L), and ground or residual heat flux (G).

function (e.g., CLASS, ISBA, and SPONSOR). Exponential functions with a maximum density are generally applied. A further increase in complexity is a parameterization based upon the physics of compactive viscosity in snow and often generalized from Kojima (1967) (e.g., BASE, CROCUS, CSIRO, and SLAM). However, as with other relations that are partly empirically derived, parameter values are not available for all conditions and may be the cause of differences when compared with observations (Slater et al. 1998). An increase in density can also occur as the result of meltwater refreezing in the snowpack (e.g., CLASS and SPONSOR). Table 2 shows there is a wide variety of methods of determining density and how energy flows through the snowpack. Sturm et al. (1997) provide a comprehensive review of methods for determining thermal conductivity. They indicate that, although it may be the easiest method for parameterization, snow density is not the fundamental controlling variable in determining thermal conductivity. Furthermore, the regressions they developed are somewhat different from those currently employed in LSSs. Both of these points deserve further attention with respect to LSSs.

5. Sensitivity to downward longwave radiation

As noted in Schlosser et al. (2000), there is variable sensitivity to the change in LWD among the models. The decrease in LWD produces a colder environment, a longer snow season, and larger SWE. It is evident that some schemes become very cold. Figure 7 shows that, over the midwinter period, turbulent fluxes of latent and sensible heat are near zero for many schemes (e.g., BASE, CLASS, SPONSOR, and SPS), and hence the surface energy balance is controlled by radiative fluxes. In the LNGW simulation (see section 2), changes in

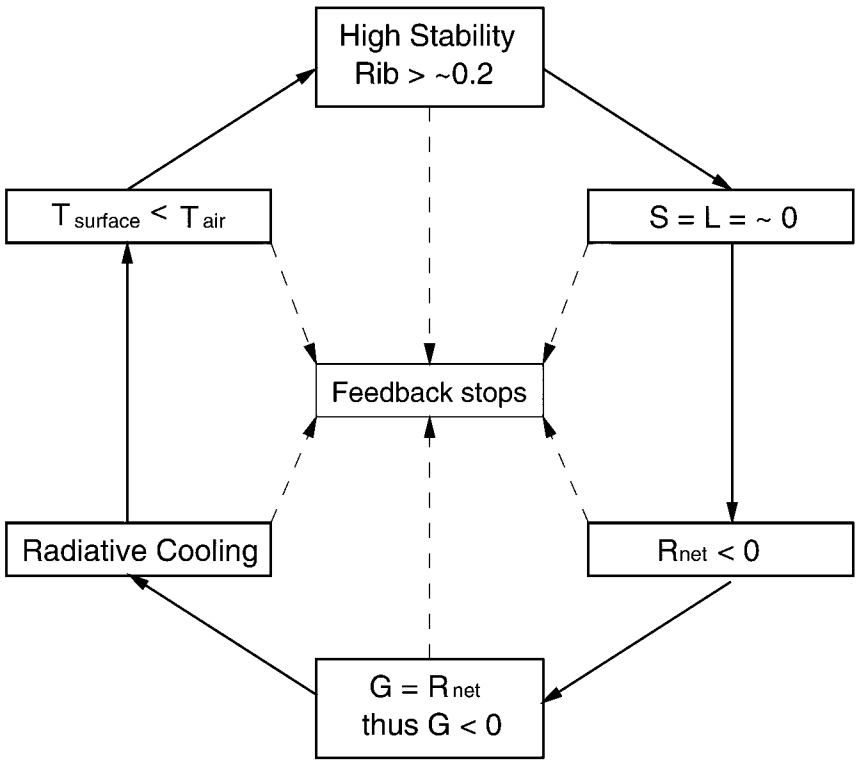

FIG. 8. The stability-induced cooling feedback illustrating a decoupling of surface and atmosphere. Solid arrows indicate that the condition in the box is true; dashed lines indicate that they are false. As the snow surface cools, more energy will later be required for melt to occur. Rnet, G, S, L, and Rib are net radiation, ground heat flux, sensible heat, latent heat, and the bulk Richardson number, respectively.

absorbed solar radiation from the CTRL simulation are negligible and the LWD difference is equal across the models. Net radiation is negative over winter in the LNGW simulation, and, with sensible heat and latent heat fluxes equal to zero in the above-mentioned models, heat is continually lost via radiation. This loss creates a positive feedback in which the ground heat flux at the surface is increasingly negative as it attempts to equal the negative net radiation (Fig. 8). The cooler surface is then used to determine outgoing radiation in the next time step. Essentially, these schemes have become decoupled from the atmosphere during midwinter. Bulk Richardson numbers (Ri_b) move above the critical value (Ri_{cr}) of ~0.2–0.25, at which point turbulent transfer virtually ceases. For example, BASE, which is not the coldest model, would produce Ri_bs in excess of 1.0 during winter nights. The sooner the surface becomes colder than the threshold of stability-induced near-zero turbulent transfer, the faster they cool, which is why we see that ''colder'' schemes are more sensitive in the LWD, and the positive feedback results in a very large difference in surface temperature over winter as compared with summer (Fig. 3b). The colder the snow becomes, the more difficult it is to melt; thus it has a longer duration and greater SWE. This problem of the land surface sensitivity or decoupling from the atmosphere under very stable conditions has been noted in other studies (Krinner et al. 1997; Derbyshire 1999; Yang et al. 1999b). A noteworthy model is BUCKET, which has no stability correction and is thus the least sensitive to LWD. Figure 3c shows that for the cold models early season ablation was reduced, but that over the midwinter period there is no increasing difference in SWE between the CTRL and LNGW simulations.

Jordan et al. (1999) discussed the use of a modified surface transfer formulation designed specifically to avoid problems of surface–atmosphere decoupling over snow-covered sea ice. They suggested a two-part solution in which Ri_{cr} is increased to 1.43 (based on observations) and a windless exchange coefficient is added on the hypothesized basis that breaking gravity wave actions can still cause some intermittent heat exchange in stable conditions. The assumptions about effective homogeneity and aggregation methods used in LSS surface transfer formulations are clearly an area deserving attention for stable cases.

Differences in aerodynamic parameterizations were shown by Desborough (1999) to be, in part, responsible for model scatter in other PILPS experiments, and, in the case of snow cover, the effect of the stability feedback increases model sensitivity. One area in which models may not be correctly following reality is snow

surface emissivity (ε_{snow}). In our experiments, ε_{snow} was set to 1.0, because snow is generally considered to be a near-blackbody radiator, with measurements suggesting emissivity values on the order of 0.97–1.00 (e.g., Kondo and Yamazawa 1986; Griggs 1968). Theoretical calculations suggest an emissivity value of 0.94–1.00, depending upon wavelength, density, and grain size (Warren 1982). However, Mellor (1977), quoting Dunkle and Gier (1955), suggests that these high values of emissivity are only associated with snow at temperatures near 0°C; colder snow (near −3°C) was found to have an emissivity as low as 0.87. Rees (1993a, b), in an investigation of Arctic snow, reported emissivity of some snow samples falling below 0.80, with very cold temperatures, for the thermal infrared portion of the spectrum (8–14 μm). The values of emissivity given by Oke (1987) are 0.82 for old snow and 0.99 for fresh snow, and, in its standard mode, AMBETI follows these values in a linear fashion. However, most models maintain a high constant value of ε_{snow} (usually 1.0). By decreasing ε_{snow} with temperature, a negative feedback is imposed upon calculations of the surface energy balance, and net radiation would not fall as low as it does, thus halting some of the decoupling of models. Determining appropriate values of ε_{snow} is an area requiring further investigation.

For those schemes that do not exhibit the stability-feedback characteristic, part of the difference in SWE is due to increased sublimation of snow to the surface in the LNGW simulation. This area is of interest (section 4a), but it is of much less significance when compared with the temperature-stability feedback mentioned above. Garratt and Prata (1995) noted that the largest discrepancy in LWD between GCMs and observations is in the polar regions, and the sensitivity displayed to LWD among the models here does not strengthen our confidence in future climate scenarios for high-latitude areas.

6. Summary and conclusions

This paper has investigated the simulation of snow by 21 land surface models. We have shown that the models as a group can capture the general patterns of accumulation and ablation on an interannual basis, but weaknesses such as midseason ablation exist. Among the models there is considerable scatter (e.g., a 40-day difference across the complete ablation of snow), but much of the scatter is systematic. In an attempt to explain this scatter, we have investigated how models make energy available to their respective snowpacks and how that energy is then distributed and used.

The combination of albedo and/or fractional cover has a large influence on the amount of energy absorbed by the snow. We have shown that the early part of the snow season, especially during ablation ''events,'' produces considerable scatter, because in such low-SWE conditions the amount of energy incident to the portion of the grid assigned as snow varies widely across the models. Scatter that occurs in the early part of the season is maintained during the winter by internal feedback processes or model-independent snowfall events. Early-season snow cover has been suggested as more influential than winter snow cover on the general circulation in the Northern Hemisphere (Cohen and Entekhabi 1999). Determining an appropriate fractional snow cover at the macroscale for all vegetation types has not yet been completely resolved through remote sensing and should be addressed.

Sublimation from or deposition to the snow surface is responsible for a proportion of the scatter among models, but this area has few observations and requires further investigation. The question of whether LSSs need to include blowing-snow parameterizations also remains unsolved.

Model structure plays an important role in determining the partitioning of energy between snow and other portions of an LSS. The implementation of similar parameterizations for a particular process (e.g., fractional cover) can have widely differing effects, depending upon structure. Alternatively, models with a similar structure for snow can show differing sensitivities, depending upon the overall composition of the model (e.g., the underlying soil model). Structure will influence thermal properties of snow, which ultimately determine temperature and ablation rates. We have also investigated the differences in parameters and parameterizations of snow thermal conductivity, emissivity, and density and noted what influence these may have on simulations.

The sensitivity of some models to LWD can be attributed to their aerodynamic formulations. The colder models can create a stability-induced shutoff of their turbulent heat fluxes, thus increasing their LWD sensitivity through a positive feedback when net radiation is negative.

The differences shown in Table 2, as well as those shown in Figs. 2 and 3, indicate that a wide variety of parameterizations are implemented with respect to snow. In addition, there is a problem across most models in that they treat snow as a simplified generic substance. Sturm et al. (1995) clearly show that there are differing characteristics associated with various forms of snow. Computational expense does not allow us to include the full physics of snow processes for global applications; thus, once a degree of empiricism is introduced via parameterizations, a model may be better suited to one particular climate dataset of snow than another. Not yet discernible is which particular combination of parameterization methods is best for a given application, but, in the context of this study we have identified those areas that produce the greatest difference in snow modeling and are most deserving of attention. Last, following preliminary discussions of results amongst participants of PILPS 2(d), several models have updated their snow parameterizations since the initiation of this pro-

ject in 1996, indicating the value of projects such as PILPS.

Acknowledgments. This work is supported by the Australian Research Council, NOAA Climate and Global Change Program Grant NA56GPO212, NASA Grants NAGW-5227 and NAG55161, and Russian Foundation for Basic Research Grants 98-05-64218 and 97-05-64467. N. A. Speranskaya's efforts in data recovery are acknowledged. Thanks to R. Essery for comments concerning UKMO and MOSES, to B. Goodison and D. Yang for comments regarding snow data at Valdai, and R. E. Davis and two anonymous reviewers for aiding clarification.

REFERENCES

Abdella, K., and N. A. MacFarlane, 1996: Parameterization of the surface-layer exchange coefficients for atmospheric models. *Bound.-Layer Meteor.,* **80,** 223–248.

Anderson, E. A., 1976: A point energy and mass balance model of a snow cover. NOAA Tech. Rep. NWS 19, U.S. Dept. of Commerce, Washington, DC, 150 pp.

Beljaars, A. C. M., and A. A. M. Holtslag, 1991: Flux parameterization over land surfaces for atmospheric models. *J. Appl. Meteor.,* **30,** 327–341.

Betts, A. K., F. Chen, K. E. Mitchell, and Z. I. Janji, 1997: Assessment of the land surface and boundary layer models in two operational versions of the NCEP Eta Model using FIFE data. *Mon. Wea. Rev.,* **125,** 2896–2916.

Bonan, G. B., 1996: A land surface model (LSM version 1.0) for ecological, hydrological, and atmospheric studies: Technical description and user's guide. NCAR Tech. Note NCAR/TN−417 + STR, 150 pp. [Available from UCAR Communications, P.O. Box 3000, Boulder, CO 80307.]

Braden, H., 1995: The model AMBETI: A detailed description of a soil–plant–atmosphere model. Berichte des Deutschen Wetterdienstes, Offenbach am Main, Nr. 195, 117 pp. [Available from Deutscher Wetterdienst, Zentralamt, Frankfurter Str. 135, 63067 Offenbach am Main, Germany.]

Brun, E., E. Martin, V. Simon, C. Gendre, and C. Coleou, 1989: An energy and mass model of snow cover suitable for operational avalanche forecasting. *J. Glaciol.,* **35** (121), 333–341.

——, P. David, and M. Sudul, 1992: A numerical model to simulate snow-cover stratigraphy for operational avalanche forecasting. *J. Glaciol.,* **38,** 13–22.

Brutsaert, W., 1975: On a derivable formula for long-wave radiation from clear skies. *Water. Resour. Res.,* **11,** 742–744.

Cess, R. D., and Coauthors, 1991: Interpretation of snow-climate feedbacks as produced by 17 general circulation models. *Science,* **253,** 888–892.

Chalita, S., and H. Le Treut, 1994: The albedo of temperate and boreal forest and the Northern Hemisphere climate: A sensitivity experiment using the LMD GCM. *Climate Dyn.,* **10,** 231–240.

Chang, A. T. C., J. L., Foster, and D. K. Hall, 1990: Satellite estimates of Northern Hemisphere snow volume. *Int. J. Remote Sens.,* **11,** 167–172.

Chen, F., and Coauthors, 1996: Modeling of land surface evaporation by four schemes and comparison with FIFE observations. *J. Geophys. Res.,* **101,** 1194–1215.

Cohen, J., and D. Rind, 1991: The effect of snow cover on the climate. *J. Climate,* **4,** 689–706.

——, and D. Entekhabi, 1999: Eurasian snow cover variability and Northern Hemisphere climate predictability. *Geophys. Res. Lett.,* **26,** 345–348.

Cox, P. M., R. A. Betts, C. B. Bunton, R. L. H. Essery, P. R. Rowntree, and J. Smith, 1999: The impact of new land surface physics on the GCM simulation of climate and climate sensitivity. *Climate Dyn.,* **15,** 183–203.

Dai, Y.-J., and Q.-C. Zeng, 1997: A land-surface model (IAP94) for climate studies, Part I: Formulation and validation in off-line experiments. *Adv. Atmos. Sci.,* **14,** 433–460.

Derbyshire, S. H., 1999: Boundary-layer decoupling over cold surfaces as a physical boundary-instability. *Bound.-Layer Meteor.,* **90,** 297–325.

de Rosnay, P., and J. Polcher, 1999: Modeling root water uptake in a complex land surface scheme coupled to a GCM. *Hydrol. Earth Syst. Sci.,* **2,** 239–255.

Desborough, C. E., 1997: The impact of root-weighting on the response of transpiration to moisture stress in a land surface scheme. *Mon. Wea. Rev.,* **125,** 1920–1930.

——, 1999: Surface energy balance complexity in GCM land surface models. *Climate Dyn.,* **15,** 389–403.

——, and A. J. Pitman, 1998: The BASE land surface model. *Global Planet. Change,* **19,** 3–18.

Dewey, K. F., 1977: Daily maximum and minimum temperature forecasts and the influence of snow cover. *Mon. Wea. Rev.,* **105,** 1594–1597.

Dickinson, R. E., A. Henderson-Sellers, and P. J. Kennedy, 1993: Biosphere–Atmosphere Transfer Scheme (BATS) Version 1e as coupled to the NCAR Community Climate Model. NCAR Tech. Note TN-387 + STR, 72 pp. [Available from UCAR Communications, P.O. Box 3000, Boulder, CO 80307.]

Douville, H., J. F. Royer, and J. F. Mahfouf, 1995: A new snow parameterization for the Météo-France climate model. 1. Validation in stand-alone experiments. *Climate Dyn.,* **12,** 21–35.

Dunkle, R. V., and J. T. Gier, 1955: Spectral characteristics of wet and dry snow between 0 and −60°C. U.S. Army Snow, Ice and Permafrost Research Establishment (US SIPRE) Tech. Rep. 16, 122 pp. [Available from Cold Regions Research and Engineering Laboratory, 72 Lyme Rd., Hanover, NH 03755.]

Essery, R., 1997: Modelling fluxes of momentum, sensible heat and latent heat over heterogeneous snow cover. *Quart. J. Roy. Meteor. Soc.,* **123,** 1867–1883.

——, 1998: Boreal forests and snow in climate models. *Hydrol. Processes,* **12,** 1561–1567.

——, E. Martin, H. Douville, A. Fernández, and E. Brun, 1999: A comparison of four snow models using observations from an alpine site. *Climate Dyn.,* **15,** 583–593.

Fedorov, S. F., 1977: *A Study of the Components of the Water Balance in Forest Zone of European Part of the USSR* (in Russian). Gidrometeoizdat, 264 pp.

Foster, J., and Coauthors, 1996: Snow cover and snow mass intercomparisons of general circulation models and remotely sensed datasets. *J. Climate,* **9,** 409–426.

Garratt, J. R., and A. J. Prata, 1996: Downwelling longwave fluxes at continental surfaces—a comparison of observations with GCM simulations and implications for the global land surface radiation budget. *J. Climate,* **9,** 646–655.

Gates, W. L., 1992: AMIP: The Atmospheric Model Intercomparison Project. *Bull. Amer. Meteor. Soc.,* **73,** 1962–1970.

Gedney, N., 1995: Development of a land surface scheme and its application to the Sahel. Ph.D. dissertation, University of Reading, 200 pp. [Available from Dept. of Meteorology, University of Reading, Reading RG6 6BB, United Kingdom.]

Giorgi, F., and R. Avissar, 1997: Representation of heterogeneity effects in earth system modeling: Experience from land surface modeling. *Rev. Geophys.,* **35** (4), 413–437.

Griggs, M., 1968: Emissivities of natural surfaces in the 8- to 14-micron spectral region. *J. Geophys. Res.,* **73,** 7545–7551.

Groisman, P. Ya., T. R. Karl, and R. W. Knight, 1994: Observed impact of snow cover on the heat balance and the rise of continental spring temperatures. *Science,* **263,** 198–200.

Gusev, Ye. M., and O. N. Nasonova, 1998: The land surface parameterization scheme SWAP: Description and partial validation. *Global Planet. Change,* **19,** 63–86.

Henderson-Sellers, A., A. J. Pitman, P. K. Love, P. Irannejad, and T.

H. Chen, 1995: The Project for Intercomparison of Land Surface Parameterization Schemes (PILPS): Phases 2 and 3. *Bull. Amer. Meteor. Soc.,* **76,** 489–503.

Hess, G. D., and B. J. McAvaney, 1998: Realisability constraints for land-surface schemes. *Global Planet. Change,* **19,** 241–245.

Idso, S. B., 1981: A set of equations for full spectrum and 8–14-m and 10.5–12.5-m thermal radiation from cloudless skies. *Water Resour. Res.,* **17** (1), 295–304.

Jordan, R. E., E. L Andreas, and A. P. Makshatas, 1999: Heat budget of snow-covered sea ice at North Pole 4. *J. Geophys. Res.,* **104,** 7785–7806.

Kim, J., and M. Ek, 1995: A simulation of the surface energy budget and soil water content over the HAPEX-MOBILHY forest site. *J. Geophys. Res.,* **100,** 20 845–20 854.

Kojima, K., 1967: Densification of seasonal snow cover. *Physics of Snow and Ice,* H. Oura, Ed., Institute of Low Temperature Science, 929–952.

Kondo, J., and H. Yamazawa, 1986: Measurement of snow surface emissivity. *Bound.-Layer Meteor.,* **34,** 415–416.

Koren, V., J. Schaake, K. Mitchell, Q.-Y. Duan, F. Chen, and J. M. Baker, 1999: A parameterization of snowpack and frozen ground intended for NCEP weather and climate models. *J. Geophys. Res.,* **104,** 19 569–19 585.

Krinner, G., C. Genthon, Z.-X. Lin, and P. Le Van, 1997: Studies of the Antarctic climate with a stretched-grid general circulation model. *J. Geophys. Res.,* **102,** 13 731–13 745.

Kukla, G., 1981: Climatic role of snow covers. *Sea Level, Ice and Climate Change,* IAHS Publication No. 131, IAHS Press, 79–107.

Lamb, H. H., 1955: Two-way relationships between the snow or ice limit and 1000–500-mb thickness in the overlying atmosphere. *Quart. J. Roy. Meteor. Soc.,* **81,** 172–189.

Leathers, D. J., and D. A. Robinson, 1993: The association between extremes in North American snow cover extent and United States temperatures. *J. Climate,* **6,** 1345–1355.

Liston, G. E., 1995: Local advection of momentum, heat and moisture during the melt of patchy snow covers. *J. Appl. Meteor.,* **34,** 1705–1715.

——, 1999: Interrelationships among snow distribution, snowmelt, and snow cover depletion: Implications for atmospheric, hydrologic and ecologic modeling. *J. Appl. Meteor.,* **38,** 1474–1487.

Loth, B., H. F. Graf, and J. M. Oberhuber, 1993: Snow cover model for global climate simulations. *J. Geophys. Res.,* **98,** 10 451–10 464.

Louis, J.-F., 1979: A parametric model of vertical eddy fluxes in the atmosphere. *Bound.-Layer Meteor.,* **17,** 187–202.

Lynch, A. H., D. L. McGinnis, and D. A. Bailey, 1998: Snow-albedo feedback and the spring transition in a regional climate system model: Influence of a land surface model. *J. Geophys. Res.,* **103,** 29 037–29 049.

Lynch-Steiglitz, M., 1994: The development and validation of a simple snow model for the GISS GCM. *J. Climate,* **7,** 1842–1855.

Manabe, S., 1969: Climate and the ocean circulation. 1. The atmospheric circulation and the hydrology of the Earth's surface. *Mon. Wea. Rev.,* **97,** 739–774.

Mellor, M., 1977: Engineering properties of snow. *J. Glaciol.,* **19,** 15–66.

Namias, J., 1985: Some empirical evidence for the influence of snow cover on temperature and precipitation. *Mon. Wea. Rev.,* **113,** 1542–1553.

Navarre, J. P., 1975: Modele unidimensionnel d'evolution de la neige deposee (A one-dimensional model of snowpack metamorphism). *Meteorologie,* **4,** 103–120.

Neumann, N., and P. Marsh, 1998: Local advection of sensible heat in the snowmelt landscape of Arctic tundra. *Hydrol. Processes,* **12,** 1547–1560.

Noilhan, J., and J. F. Mahfouf, 1996: The ISBA land surface parameterization scheme. *Global Planet. Change,* **13,** 145–159.

Oke, T. R., 1987: *Boundary Layer Climates.* 2d ed. Routledge, 435 pp.

Pan, Z., S. G. Benjamin, J. M. Brown, and T. Smirnova, 1994: Comparative experiments with MAPS on different parameterization schemes for surface moisture flux and boundary layer processes. *Mon. Wea. Rev.,* **122,** 449–470.

Pomeroy, J. W., and R. L. H. Essery, 1999: Turbulent fluxes during blowing snow: Field tests of model sublimation predictions. *Hydrol. Processes,* **13,** 2963–2975.

——, D. M. Gray, K. R. Shook, B. Toth, R. L. H. Essery, A. Pietroniro, and N. Hedstrom, 1998: An evaluation of snow accumulation and ablation processes for land surface modelling. *Hydrol. Processes,* **12,** 2339–2367.

Randall, D. A., and Coauthors, 1994: Analysis of snow feedbacks in 14 general circulation models. *J. Geophys. Res.,* **99,** 20 757–20 771.

Rees, W. G., 1993a: Infrared emissivities of Arctic land cover types. *Int. J. Remote Sens.,* **14,** 1013–1017.

——, 1993b: Infrared emissivity of Arctic winter snow. *Int. J. Remote Sens.,* **14,** 3069–3073.

Robinson, D. A., K. F. Dewey, and R. R. Heim, 1993: Global snow cover monitoring: An update. *Bull. Amer. Meteor. Soc.,* **74,** 1689–1696.

Robock, A., 1983: Ice and snow feedbacks and the latitudinal and seasonal distribution of climate sensitivity. *J. Atmos. Sci.,* **40,** 986–997.

——, K. Ya. Vinnikov, C. A. Schlosser, N. A. Speranskaya, and Y. Xue, 1995: Use of midlatitude soil moisture and meteorological observations to validate soil moisture simulations with biosphere and bucket models. *J. Climate,* **8,** 15–35.

Schimel, D. S., B. H. Braswell, E. A. Holland, R. McKeown, D. S. Ojima, T. H. Painter, W. J. Parton, and A. R. Townsend, 1994: Climatic, edaphic, and biotic controls over storage and turnover of carbon in soils. *Global Biogeochem. Cycles,* **8,** 279–293.

Schlosser, C. A., A. Robock, K. Ya. Vinnikov, N. A. Speranskaya, and Y. Xue, 1997: 18-year land surface hydrology model simulations for a midlatitude grassland catchment in Valdai, Russia. *Mon. Wea. Rev.,* **125,** 3279–3296.

——, and Coauthors, 2000: Standalone simulations of a boreal hydrology with land surface schemes used in atmospheric models: PILPS Phase 2(d). *Mon. Wea. Rev.,* **128,** 301–321.

Sellers, P. J., and Coauthors, 1996: A revised land surface parameterization (SiB2) for atmospheric GCMs. Part I: Model formulation. *J. Climate,* **9,** 676–705.

——, and Coauthors, 1997: BOREAS in 1997: Experiment overview, scientific results, and future directions. *J. Geophys. Res.,* **102,** 28 731–28 769.

Shmakin, A. B., 1998: The updated version of SPONSOR land surface scheme: PILPS-influenced improvements. *Global Planet. Change,* **19,** 49–62.

Slater, A. G., A. J. Pitman, and C. E., Desborough, 1998: The validation of a snow parameterization designed for use in general circulation models. *Int. J. Climatol.,* **18,** 595–617.

Smirnova, T. G., J. M. Brown, and S. G. Benjamin, 1997: Performance of different soil model configurations in simulating ground surface temperature and surface fluxes. *Mon. Wea. Rev.,* **125,** 1870–1884.

——, ——, ——, and D. Kim, 2000: Parameterization of cold-season processes in the MAPS land-surface scheme. *J. Geophys. Res.,* **105,** 4077–4086.

Sturm, M., and J. Holmgren, 1998: Differences in compaction behavior of three climate classes of snow. *Ann. Glaciol.,* **26,** 125–130.

——, ——, and G. E. Liston, 1995: A seasonal snow cover classification system for local to global applications. *J. Climate,* **8,** 1261–1283.

——, ——, M. Konig, and K. Morris, 1997: The thermal conductivity of seasonal snow. *J. Glaciol.,* **43,** 26–41.

Sud, Y. C., and D. M. Moko, 1999: New snow-physics to complement SSiB. Part 1: Design and evaluation with ISLSCP Initiative 1 datasets. *J. Meteor. Soc. Japan.,* **77,** 349–366.

Tait, A. B., 1998: Estimation of snow water equivalent using passive microwave radiation data. *Remote Sens. Environ.*, **64,** 286–291.

Tao, X., J. E., Walsh, and W. L. Chapman, 1996: An assessment of global climate model simulations of Arctic air temperatures. *J. Climate*, **9,** 1060–1076.

Tilley, J. S., and A. H. Lynch, 1998: On the applicability of current land surface schemes for Arctic tundra: An intercomparison study. *J. Geophys. Res.*, **103,** 29 051–29 063.

Vernekar, A. D., J. Zhou, and J. Shukla, 1995: The effect of Eurasian snow cover on the Indian monsoon. *J. Climate*, **8,** 248–266.

Verseghy, D. L., 1991: CLASS—a Canadian land surface scheme for GCMs. I. Soil model. *Int. J. Climatol.*, **11,** 111–133.

Vinnikov, K. Ya., A. Robock, N. A. Speranskaya, and C. A. Schlosser, 1996: Scales of temporal and spatial variability of midlatitude soil moisture. *J. Geophys. Res.*, **101,** 7163–7174.

Viterbo, P., and A. C. Beljaars, 1995: An improved land surface parameterization scheme in the ECMWF model and its validation. *J. Climate*, **8,** 2716–2748.

——, and A. K. Betts, 1999: The impact on ECMWF forecasts to changes to the albedo of the boreal forests in the presence of snow. *J. Geophys. Res.*, **104,** 19 361–19 366.

——, A. Beljaars, J. F. Mahfouf, and J. Teixeira, 1999: The representation of soil moisture freezing and its impact on the stable boundary layer. *Quart. J. Roy. Meteor. Soc.*, **125,** 2401–2426.

Warren, S. G., 1982: Optical properties of snow. *Rev. Geophys. Space Phys.*, **20,** 67–89.

——, and W. J. Wiscombe, 1980: A model for the spectral albedo of snow. II: Snow containing atmospheric aerosols. *J. Atmos. Sci.*, **37,** 2734–2745.

Warrilow, D. A., and E. Buckley, 1989: The impact of land surface processes on the moisture budget of a climate model. *Ann. Geophys.*, **7,** 439–450.

Wetzel, P., and A. Boone, 1995: A parameterization for land–atmosphere–cloud exchange (PLACE): Documentation and testing of a detailed process model of the partly cloudy boundary layer over heterogeneous land. *J. Climate*, **8,** 1810–1837.

Wiscombe, W. J., and S. G. Warren, 1980: A model for the spectral albedo of snow. I: Pure snow. *J. Atmos. Sci.*, **37,** 2712–2733.

Xue, Y., P. J. Sellers, J. L. Kinter, and J. Shukla, 1991: A simplified biosphere model for global climate studies. *J. Climate*, **4,** 345–364.

——, F. J. Zeng, and C. A. Schlosser, 1996: SSiB and its sensitivity to soil properties—a case study using HAPEX–Mobilhy data. *Global Planet. Change*, **13,** 183–194.

Yang, D., J. R. Metcalfe, B. E. Goodison, and E. Mekis, 1996: Adjustment for undercatch of the double fence intercomparison reference (DFIR) gauge. Annex 2.H, WMO Solid Precipitation Measurement Intercomparison Final Rep., Instruments and Observing Methods Rep. 67, WMO/TD 872, 305 pp.

Yang, Z. L., R. E. Dickinson, A. Robock, and K. Ya. Vinnikov, 1997: On validation of the snow sub-model of the biosphere–atmosphere transfer scheme with Russian snow cover and meteorological observational data. *J. Climate*, **10,** 353–373.

——, G.-Y. Niu, and R. E. Dickinson, 1999a: Comparing snow simulations from NCAR LSM and BATS using PILPS 2d data. *Preprints, 14th Conf. on Hydrology*, Dallas, TX, Amer. Meteor. Soc., 316–319.

——, and Coauthors, 1999b: Simulation of snow mass and extent in general circulation models. *Hydrol. Processes*, **13,** 2097–2113.

Yeh, T.-C., R. T. Wetherald, and S. Manabe, 1983: A model study of the short-term climatic and hydrologic effects of sudden snow-cover removal. *Mon. Wea. Rev.*, **111,** 1013–1024.

Yen, Y.-C., 1981: Review of thermal properties of snow, ice and sea ice. CRREL Rep. 81-10, 27 pp. [Available from Cold Regions Research and Engineering Laboratory, 72 Lyme Rd., Hanover, NH 03755.]

Yosida, Z., 1955: Physical studies on deposited snow. *Contrib. Inst. Low Temp. Sci.*, **7,** 19–74.